Relationships among Forearc Structure, Fault Slip, and Earthquake Magnitude: Numerical Simulations with Applications to the Central Chilean Margin

Xiaoyu Wang[1], Julia K. Morgan[1], Nathan Bangs[2]

[1] Department of Earth, Environmental and Planetary Sciences, Rice University, Houston, Texas, USA.

[2] Institute for Geophysics, University of Texas at Austin, Austin, USA

Corresponding author: Xiaoyu Wang (xw33@rice.edu)

Key Points:

Dimensions and frictional properties of the outer wedge affect earthquake magnitude and slip distribution.

The 1960 Valdivia earthquake likely experienced its highest slip close to the trench.

Future seismic hazards may be predicted early by determining forearc structures.

Keywords

Discrete element models, South Central Chile Margin, Megathrust Earthquake, Friction, Outer Wedge, Coseismic Slip, Seismic Hazard Assessment

Abstract

Two adjacent segments of the Chile margin exhibit significant differences in the earthquake magnitude and rupture extents, reflected by the 1960 Valdivia and 2010 Maule earthquake. In this study, we use the Discrete Element Method to explore the controls on megathrust fault slip during the earthquake, informed by interpretations of the structure across these two segments. We simulate the upper plate as wedges overlying megathrust faults that are divided into two frictional domains, modeled after dynamic Coulomb wedge models. We find that the inner wedge width strongly influences megathrust rupture extents. Our selected model yields a reasonable fit to the published slip distributions for the 2010 Maule rupture. Our simulated slip distributions suggest that the Valdivia earthquake likely experienced its highest slip close to the trench, differing from published models. We also demonstrate how the frictional conditions beneath the outer wedge can affect the size of megathrust earthquakes.

Plain Language Summary

The South-central Chilean margin is host to some of the largest megathrust earthquakes on Earth, including the Mw 9.5 1960 Valdivia earthquake and the Mw 8.8 2010 Maule earthquake. Although their earthquake rupture segments are very close to each other, the resulting earthquakes are significantly different. In this study, we use the Discrete Element Method to explore the controls on these differences. We use assemblages of discrete particles to simulate wedges that define the two-dimensional subduction upper plate. Each wedge is partitioned into a strong inner wedge, capable of supporting large elastic strains that can be released during earthquakes, and a lower strength frontal domain that resists the earthquake rupture. We simulate earthquake unloading by instantaneously reducing the basal friction beneath the inner wedge, then document the resulting changes in geometry and stress throughout the wedge. We find that the dimensions and frictional properties of the frontal domain affect earthquake size. Our models yield reasonable fits to the modeled slip distributions for the 2010 Maule rupture. However, differences between the Valdivia earthquake rupture models and our simulated slip distributions suggest that the highest, slip during the earthquake, occurred close to the trench, in contrast to published models.

1 Introduction

The South-central Chilean subduction margin is host to some of the largest megathrust earthquakes on Earth, including the greatest ever recorded earthquake, the Mw 9.5 1960 Valdivia earthquake. The largest earthquake along the margin since then was the Mw 8.8 2010 Maule earthquake, which partially overlaps and extends farther north from the Valdivia rupture (Figure 1a). Despite the proximity of the two source areas, the earthquake magnitudes, rupture extents, and efficiency of generating transoceanic tsunamis differ significantly between the 1960 and 2010 events. The 1960 Valdivia event ruptured a length of ~1000 km of the Nazca-South America plate boundary along the strike from 37°S to 46°S (Figure 1a). The subsequent trans-Pacific tsunami was so large that waves up to 25 m high reached the coast of Chile (Moreno *et al.*, 2009; Contreras-Reyes *et al.*, 2010). By comparison, the 2010 Maule earthquake ruptured a length of ~600 km from 33°S to 39°S (Figure 1a), producing a much smaller tsunami with average waves of 10 m (Contreras-Reyes *et al.*, 2010; Moreno *et al.*, 2010). In addition, the maximum coseismic slip triggered by the 1960 Valdivia earthquake was over 40 m (Moreno *et al.*, 2009), whereas the maximum slip accompanying the 2010 Maule earthquake was estimated to be ~20 m (Moreno *et al.*, 2010; Tong *et al.*, 2010). Furthermore, fault slip models for the 2010 Maule earthquake rupture suggested that the rupture did not extend to the trench (Delouis *et al.*, 2010; Moreno *et al.*, 2010; Tong *et al.*, 2010; Maksymowicz *et al.*, 2017). In contrast, although dependent on poor quality data, tsunami models and joint displacement inversions suggested trench-breaking coseismic rupture for the 1960 Valdivia earthquake (Barrientos and Ward, 1990; Moreno *et al.*, 2009).

A plausible explanation for the difference in earthquake magnitudes and slip distributions for these two events is along strike variations in the position of the updip seismic-aseismic transition, and associated controls on earthquake magnitude (Wang and Hu, 2006; Contreras-Reyes *et al.*, 2010). As shown in Figure 1b, the overlying forearc theoretically can be divided into outer and inner wedges (Wang and Hu, 2006). The outer wedge, composed of relatively young unconsolidated sediments, may define a velocity strengthening zone during earthquakes (Scholz, 1998; Moore and Saffer, 2001). The inner wedge, consisting of older and stronger accreted sediments and rock, is more prone to fault locking during the interseismic period, and velocity weakening during earthquake ruptures (Wang and Hu, 2006). The boundary between the inner and outer wedge can be defined by the location of the backstop (Contreras-Reyes *et al.*, 2010). Contreras-Reyes *et al.* (2010) interpreted that the dimension of the outer wedge in the 1960 rupture area is much smaller than the one in the 2010 rupture area (Table S1, Supporting Information). Hence, there is an inverse correlation between the outer wedge dimension and earthquake size (Wang and He, 2008; Contreras-Reyes *et al.*, 2010; Contreras-Reyes *et al.*, 2017). However, this hypothesis is based on limited data and uncertain interpretations of both wedge width and earthquake slip. In particular, there are significant uncertainties about the true slip distributions for the earthquakes (Langer, 2020). Furthermore, limited coverage and poor-quality seismic records for the 1960 Valdivia earthquake make the derived slip distribution further questionable.

Another factor that may play a key role in controlling the magnitude of the coseismic rupture is the change in effective friction along the megathrust fault (Wang and Morgan, 2019). In particular, the lateral variations in fault strength beneath the outer wedge may influence the earthquake rupture behavior (Hu and Wang, 2008). However, we still have limited understanding of the relative effects of frictional behavior and outer wedge width in determining earthquake magnitude, and which may be responsible for the differences between the ruptures along the Valdivia and Maule segments.

Building on recent modeling efforts investigating the controls on distributed extensional deformation in the Japan Trench forearc following the Tohoku earthquake (Wang and Morgan, 2019), we use numerical simulations to understand potential connections between great megathrust earthquakes, fault properties, and upper plate structure. This study seeks to 1) determine the effect of position of the inner to outer wedge transition on earthquake slip distribution for comparison to the 1960 Valdivia rupture; and 2) explore how frictional changes beneath the outer wedge interact with outer wedge width to influence the magnitude of fault slip.

2 Approach and Methodology

RICEBAL, a Discrete-Element-method based program, is used to construct the models used here. Details about the DEM methodology can be found in the supplementary materials, as well as previous publications (Morgan, 2015; Wang and Morgan, 2019). The particle sizes and their mechanical properties are tabulated in the supplementary materials (S1).

The initial wedge is constructed by randomly generating particles within a two-dimensional 200 km wide domain and letting them settle under gravity. The settled particles are then sculpted to the desired wedge shape with a starting taper angle of 12° (α+β), based on published geometries for the SC Chile Margin (Maksymowicz, 2015), and subjected to gravity tilted at an angle of 8° from the vertical, simulating a fixed megathrust dip angle (β) of 8°. The initial full length of the wedge is 200 km, comparable to the downdip rupture distance along the central Chile Margin (Figure 1a). Following particle deposition and wedge sculpting, bonds are added between particles in contact within the wedge to impart cohesion.

The wedge is divided into inner and outer wedge domains, distinguished by the assigned values of basal friction on the underlying megathrust fault (Figure 1c). The mechanical properties of the domains and interfaces are controlled by the particle properties and interparticle friction coefficients assigned for each domain. The derivation of the bulk internal friction (μ'_{int}) and basal friction (μ'_{bas}) of the inner and outer wedges, respectively (Table S2, Supporting Information), is explained in the supplementary materials and previous studies (Morgan, 2015; Wang and Morgan, 2019). We use a highly simplified model that focuses on the first-order effects of fault properties and outer wedge dimension on earthquake sizes during an earthquake cycle. Therefore, we employ constant values of basal friction across each of the inner or outer wedges for a given simulation stage, ignoring the spatial and temporal variations that likely occur in nature. The resulting model, partitioned into an inner and outer wedge, is referred to as State 0.

Each numerical simulation is carried out in two stages: (1) pre-earthquake loading under enhanced "static" basal friction values, representing the interseismic period, and (2) dynamic earthquake rupture under reduced basal friction beneath the inner wedge. This friction change is a simplified way to simulate velocity-weakening, thought to accompany great earthquakes within the subduction seismogenic zones, theoretically causing rupture propagation or even extensional failure (Wang and Hu, 2006; Wang and Morgan, 2019). In combination, the two stages approximate a full earthquake cycle. During the first stage, the backwall (positioned at 0 km) is displaced at a steady rate, while the slip of the wedge is resisted by basal friction. This causes the build-up of elastic strain energy within the wedge and increased shear stresses along the megathrust. State 1 is reached following 8 km of backwall displacement, when the fault is preconditioned and poised for failure. Earthquake rupture is induced during Stage 2 by rapidly decreasing the basal friction beneath the inner wedge, which results in dynamic slip along the underlying fault. Concurrently, the basal friction beneath the outer wedge was either maintained or increased, simulating a more resistant frontal wedge. State of the model is achieved once Stage 2 slip ceases. More information about the modeling workflow can be found in the supplementary materials (S2) and the previous work (Wang and Morgan, 2019).

We carried out two different simulation setups, each one using different combinations of basal friction and friction changes for a range of different outer wedge dimensions, as shown in Table S2 (Supporting Information). In all models, the internal friction coefficient (μ'_{int}) was maintained at 0.10 for both the inner and outer wedges.

Our first model setup (Table S1, Supporting Information) was designed to determine how the dimension of the outer wedge (velocity strengthening zone) affects the distribution of fault slip during earthquake rupture. The effective basal friction coefficients for the inner and outer wedges, μ'_{bas_inner} and μ'_{bas_outer}, respectively, were both set to 0.04 at the start of the pre-earthquake loading stage. During the earthquake rupture phase, μ'_{bas_inner} was instantly decreased to 0.02 while μ'_{bas_outer} was maintained at 0.04. Simulations were conducted for a range of outer wedge dimensions, ranging from 0% - ~60% of the full wedge length.

The second model setup (Table S2, Supporting Information) was used to investigate how the magnitude of friction, beneath the outer wedge and whether it increases or decreases during earthquake rupture, controls earthquake magnitude and resulting fault slips. As above, the effective basal friction values for both the inner and outer wedges, μ'_{bas_inner} and μ'_{bas_outer} respectively, were initially assigned to 0.04 during the pre-earthquake loading stage. Then during the earthquake rupture phase, μ'_{bas_inner} was instantly decreased to 0.02 to simulate velocity weakening, while μ'_{bas_outer} was changed to different values, ranging from 0.04 to 0.08.

3 Simulation Results

The instantaneous reduction in basal friction beneath the inner wedge allowed the simulated wedge to slip along the fixed lower plate as it unloaded, interacting with the outer wedge, which also had the potential to slip and unload. The final coseismic slip distributions for both inner and outer wedges were calculated by tracking average particle displacements within 2000×1000 m domains immediately above the fault zone.

For Setup 1, seventeen simulations were conducted using different ratios of outer wedge length to full wedge length, ranging from 0% to ~60%; the final displacements, from the backwall (at 0 km) to the wedge toe, at the end of unloading are summarized in Figure 2a-2b. A clear pattern emerges, revealing a trend of increasing local fault displacement from near the backwall to the toe, until slip is suppressed by the presence of the resistant outer wedge. Thus, we see that the distance to the peak coseismic fault displacement correlates inversely with the width of the outer wedge, and slip magnitude decreases noticeably near the transition from the inner to the outer wedge (Figure 2a). The peak slip occurs very close to the toe if the outer wedge is very small, i.e., less than 10% of the megathrust fault length (Figure 2a) but shifts away from the toe as the outer wedge width increases. Lastly, the maximum slip magnitude increases exponentially as the dimension of the outer wedge decreases (Figure 2b). A small step in displacement noted on each curve at ~40 km reflects reactivation of a fault that formed during the interseismic loading stage (Figure 1c), as is explained in the supplementary material; this fault does not contribute significantly to the rupture distribution.

With Setup 2, we compared three different outer wedge widths, and examined the effects of four different friction changes beneath the outer wedge (Figure 2c, d, and e). We see that the magnitude friction, and whether it increases or decreases, influences the cumulative fault slip, defined as the area under the slip-displacement curve. Again, in Figure 2c-2e, all models exhibit a step-in slip magnitude near the boundary between the inner and outer wedges, however, the larger the reduction in outer wedge friction, the greater the cumulative fault slip. For μ'_{bas_outer} larger than 0.04 (i.e., velocity strengthening), the coseismic slip distributions beneath the outer wedge are similar and small (blue dashes and pink circles in Figure 2c-2e). In the case of constant velocity (μ'_{bas_outer} = 0.04, black line), the outer wedge experiences higher fault slip. As above, the step-in displacement at ~40 km is due to a pre-existing fault.

4 Discussion

4.1 Controls on Earthquake Magnitudes and Coseismic Slips

We can select the results of our Setup 1 simulations that produce fault slip distributions that reasonably match both the 1960 Valdivia and 2010 Maule earthquakes. Shown in Figures 3a and b (left panels), are the selected simulation results (solid lines) that best fit the published constraints discussed previously (dashed lines). For comparison, we also revisit modeled slip distributions for the recent well-instrumented 2011 Tohoku earthquake off Japan, which is known to have ruptured all the way to the trench (Figure 3c, left panel). For each of the preferred slip distributions, we also plot corresponding model-derived stress changes that accompanied the simulated earthquakes (Figure 3d-3f, right panels), to demonstrate the role of the frictionally stronger outer wedges in modulating fault slip. The calculation of stress changes, documented as cumulative changes in mean stress, σ_m during earthquake unloading, is explained in the supplementary materials (S3). In all cases, the earthquake causes a reduction in inner wedge stress, some of which is transferred toward the toe, resulting in an increase in stress within the outer wedge. We discuss each case further below.

Based on the previous interpretation based on the tomographic model for the 2010 Mw 8.8 Maule earthquake rupture segment (Contreras-Reyes *et al.*, 2010; Contreras-Reyes *et al.*, 2017), the outer wedge zone is thought to be relatively large, and the modeled peak slip is about 20 m (Table S1, Supporting Information). Our model with an outer wedge that is ~49 % of the subduction interface and an outer wedge friction value of 0.04, matches these constraints well (Figure 3a). The case where the outer wedge is ~ 49% of the subduction interface provides a reasonable match to the estimated slip distribution. The simulated and calculated coseismic slip distributions are compared in the left panel of Figure 3a; the simulated co-seismic stress change is shown in the right panel. The peak slip from our numerical simulation (black curve) is about 21 m, centered ~ 100 km from the trench. This is consistent with the derived slip distributions (blue dash curve) for the 2010 Maule earthquake (Moreno *et al.*, 2010). The average slip is about 9.5 m, and if we assume an along strike rupture distance of 550 km (Moreno *et al.*, 2010), the moment magnitude (M_w) can be calculated as:

$$Mw = 2/3 \times \log (\mu \times \text{rupture area} \times \text{slip length}) - 10.73$$

using a standard shear modulus, μ for the crust of 3×10^{10} N/m. This yields an earthquake magnitude of around 8.8, which matches that of the Maule earthquake. The simulated coseismic stress change shows that unloading of the inner wedge transferred significant stress into the outer wedge, around 120 km, near the boundary with the inner wedge, whereas the toe of the wedge experienced essentially no change in stress. This demonstrates that the outer wedge resisted megathrust slip, limiting rupture propagation to the trench, which is consistent with expected velocity-strengthening behavior and observations that the Maule rupture did not propagate to the trench (Contreras-Reyes *et al.*, 2010; Delouis *et al.*, 2010; Moreno *et al.*, 2010; Ryder *et al.*, 2012; Maksymowicz *et al.*, 2017). In reality, the frictional transition between the inner and outer wedge in nature is probably more gradational than we have simulated here, which can explain the more gradual decrease in slip towards the toe documented for the Maule event. Nevertheless, the coseismic slip distribution derived from our simplified model, in general, agrees with previous estimates for the width of the outer wedge, as well as the coseismic slip distribution related to the 2010 Maule earthquake (Contreras-Reyes *et al.*, 2010; Moreno *et al.*, 2010; Tong *et al.*, 2010).

By comparison, the Valdivia rupture segment is thought to have a much smaller outer wedge, based on recent seismic interpretations (Contreras-Reyes *et al.*, 2010; Bangs *et al.*, 2020). The simulation with an outer wedge of 10% of the subduction interface provides a reasonable fit (Figure 3b, left panel), although with some informative differences. The peak coseismic slip from our simulations is ~45 m, comparable to the peak slip of ~44 m derived for the 1960 Valdivia earthquake (Moreno *et al.*, 2009). The average modeled slip for this case is about 22 m. If the along strike rupture distance is 1000 km (Moreno *et al.*, 2009), this yields an earthquake magnitude of ~9.4. As seen in the right panel of Figure 3e, the wedge experienced primarily coseismic stress drop, except very near the toe of the wedge, where a stress rise is observed above the strong outer wedge fault. However, despite the outer wedge resistance, our simulations suggest that the toe experienced more than 30 m of slip (Figure 3b, left panel). These slip values are consistent with previous studies that suggested the highest slip of the 1960 earthquake was over twice the peak slip triggered by the 2010 earthquake, and that the earthquake ruptured all the way to the trench (Moreno *et al.*, 2009; Contreras-Reyes *et al.*, 2010). In our simplified simulation, the highest slip patch is very close to the trench (~20 km for the black curve in Figure 3b, left panel), in contrast to the derived peak for the earthquake occurs ~100 km from the trench (green curve in Figure 3b, left panel), and suggests very little slip at the toe.

To better understand the discrepancies between our simulated displacements and the derived coseismic slip distribution for the 1960 Valdivia earthquake, we look to the 2011 Tohoku-oki earthquake, Mw is 9.0, as a good analogue. This earthquake ruptured all the way to the trench (Ide *et al.*, 2011; Ito *et al.*, 2011; Tsuji *et al.*, 2011), and the highest coseismic slip was ~ 64 m very close to the trench (Tsuji *et al.*, 2011; Wei *et al.*, 2012; Sun *et al.*, 2017). This slip distribution is more consistent with our simulation with a very small outer wedge, i.e., less than 5% of the full wedge dimension (Figure 3c). In this case, the stress decreased throughout the wedge, as the small outer wedge offered little resistance to slip. Thus, the earthquake rupture propagated all the way to the trench, with the peak slip patch very close to the trench. Considering that the magnitude of the 1960 Valdivia event was even larger than the 2011

Tohoku earthquake, the slip distribution triggered by the 1960 earthquake was perhaps more comparable to that of the 2011 Tohoku-oki earthquake. Furthermore, we infer that the highest slip patch for the 1960 earthquake was probably much closer to the trench than previously interpreted (Moreno *et al.*, 2009), but the true slip distribution was not well resolved due to the limited capabilities and distribution of seismometers at the time.

4.2 Effects of Velocity Strengthening on Coseismic Ruptures

Our results from Setup 2 provide further insights into how spatial and temporal variations in fault strength during earthquakes can influence earthquake rupture behavior. Figure 2c-2e demonstrate how coseismic changes in outer wedge friction affect the slip distribution and magnitude. If the outer wedge experiences coseismic strengthening (i.e., basal friction increases from 0.04 to 0.06-0.08) as inferred in Wang and Hu (2006) model, this results in a ~25% reduction in the magnitude of outer wedge slip, reflecting the increased fault resistance. The peak slip magnitude is also slightly reduced, most noticeably for the smallest outer wedge (Figure 2e).

The trends revealed by all these simulations demonstrate that both dimension and frictional properties of an outer wedge will play a significant role in how slip is distributed across a megathrust fault during an earthquake, and whether the rupture can extend all the way to the toe, where it might generate a large tsunami. A large outer wedge that is frictionally strong resists seaward slip and absorbs much of the stress released from the inner wedge during an earthquake, limiting displacement at the wedge toe.

5 Conclusions

Our simulations demonstrate that both the dimension and the frictional properties of the outer wedge affects earthquake magnitude, slip distribution and rupture extents. Our simulated slip distributions yield important insights into the wedge properties and frictional changes that accompanied the 2010 Maule earthquake and the 1960 Valdivia earthquake rupture, along the central Chile margin, as well as for the 2011 Tohoku-oki earthquake off Japan. With the constraints by the published peak slip, dimension of the outer wedge, as well as plausible values of megathrust friction during pre-earthquake loading and coseismic earthquake rupture, our models show consistency with the published coseismic slip distribution for the 2010 Maule and 2011 Tohoku-oki earthquake. In contrast, our simulation results imply the discrepancies between our simulated displacements and the derived coseismic slip distribution for the 1960 Valdivia earthquake. The weak match between the derived Valdivia slip model and our preferred simulation, leads us to suggest that in reality the highest slip patch probably occurred much closer to the trench, rather than ~100km away as has been suggested (Moreno *et al.*, 2009). This conclusion is supported by new evidence for the maximum slip at the toe for the well-instrumented Tohoku-oki earthquake (Ide *et al.*, 2011; Sun *et al.*, 2017).

The parameter study carried out using Setup 1 demonstrates that seismic hazards can be identified and accessed much more easily by determining the forearc structure. An interpretation of forearc structure bundled with corresponding numerical simulations can constrain the coseismic slip distributions for poorly instrumented earthquakes. Moreover, the numerical simulations, calibrated to match available slip distributions and the estimated dimensions of the frontal wedge, can be used to run parameter tests to create a template showing the correlation among the dimension of the outer wedge, coseismic rupture, and the slip distributions for various coseismic friction changes. This template could allow us to quickly predict earthquake sizes for different localities lacking records of megathrust earthquake, assuming the geometry of the frontal wedge can be estimated.

Simulation Setup 2 further shows that the magnitude of the earthquake is sensitive to frictional changes during fault rupture. The outer wedge frictional behavior can play a significant role in controlling peak slip and earthquake magnitude when the dimension of the outer wedge is sufficiently small, such as in the Valdivia rupture segment. Combining estimates of the dimensions and basal frictional changes of the outer wedges, therefore, can help us better predict the future sizes of the earthquakes and their risks.

Acknowledgments and Data

This work was funded in part by National Science Foundation grant EAR-1723249. Computing facilities were made available in part through the Rice Center for Computational Geophysics. Interested parties are encouraged to contact the author to request copies of animated GIFs of the simulations for further study. The modeling results, corresponding files, raw data, and sample code for this research can be found in the published dataset 10.6084/m9.figshare.13565447

References

Bangs, N., Morgan, J., Tréhu, A., Contreras-Reyes, E., Arnulf, A., Han, S., Olsen, K., and Zhang, E. (2020), Basal Accretion Along the South Central Chilean Margin and Its Relationship to Great Earthquakes, *Journal of Geophysical Research: Solid Earth*, *125*(11), e2020JB019861.

Barrientos, S. E., and Ward, S. N. (1990), The 1960 Chile earthquake: inversion for slip distribution from surface deformation, *Geophysical Journal International*, *103*(3), 589-598.

Contreras-Reyes, E., Maksymowicz, A., Lange, D., Grevemeyer, I., Muñoz-Linford, P., and Moscoso, E. (2017), On the relationship between structure, morphology and large coseismic slip: A case study of the Mw 8.8 Maule, Chile 2010 earthquake, *Earth and Planetary Science Letters*, *478*, 27-39.

Contreras-Reyes, E., Flueh, E. R., and Grevemeyer, I. (2010), Tectonic control on sediment accretion and subduction off south central Chile: Implications for coseismic rupture processes of the 1960 and 2010 megathrust earthquakes, *Tectonics*, *29*(6).

Delouis, B., Nocquet, J. M., and Vallée, M. (2010), Slip distribution of the February 27, 2010 Mw= 8.8 Maule earthquake, central Chile, from static and high-rate GPS, InSAR, and broadband teleseismic data, *Geophysical Research Letters*, *37*(17).

Hu, Y., and Wang, K. (2008), Coseismic strengthening of the shallow portion of the subduction fault and its effects on wedge taper, *Journal of Geophysical Research: Solid Earth*, *113*(B12).

Ide, S., Baltay, A., and Beroza, G. C. (2011), Shallow dynamic overshoot and energetic deep rupture in the 2011 Mw 9.0 Tohoku-Oki earthquake, *Science*, *332*(6036), 1426-1429.

Ito, Y., Tsuji, T., Osada, Y., Kido, M., Inazu, D., Hayashi, Y., Tsushima, H., Hino, R., and Fujimoto, H. (2011), Frontal wedge deformation near the source region of the 2011 Tohoku-Oki earthquake, *Geophysical Research Letters*, *38*(7).

Langer, L. (2020), Impact of Topography on Coseismic Modeling and Earthquake Static Slip Inversions, Princeton University.

Maksymowicz, A. (2015), The geometry of the Chilean continental wedge: Tectonic segmentation of subduction processes off Chile, *Tectonophysics*, *659*, 183-196.

Maksymowicz, A., Chadwell, C., Ruiz, J., Tréhu, A., Contreras-Reyes, E., Weinrebe, W., Díaz-Naveas, J., Gibson, J., Lonsdale, P., and Tryon, M. (2017), Coseismic seafloor deformation in the trench region during the Mw8. 8 Maule megathrust earthquake, *Scientific reports*, *7*(1), 1-8.

Moore, J. C., and Saffer, D. (2001), Updip limit of the seismogenic zone beneath the accretionary prism of southwest Japan: An effect of diagenetic to low-grade metamorphic processes and increasing effective stress, *Geology*, *29*(2), 183-186.

Moreno, M., Rosenau, M., and Oncken, O. (2010), 2010 Maule earthquake slip correlates with pre-seismic locking of Andean subduction zone, *Nature*, *467*(7312), 198-202.

Moreno, M. S., Bolte, J., Klotz, J., and Melnick, D. (2009), Impact of megathrust geometry on inversion of coseismic slip from geodetic data: Application to the 1960 Chile earthquake, *Geophysical Research Letters*, *36*(16).

Morgan, J. K. (2015), Effects of cohesion on the structural and mechanical evolution of fold and thrust belts and contractional wedges: Discrete element simulations, *Journal of Geophysical Research: Solid Earth*, *120*(5), 3870-3896.

Ryder, I., Rietbrock, A., Kelson, K., Bürgmann, R., Floyd, M., Socquet, A., Vigny, C., and Carrizo, D. (2012), Large extensional aftershocks in the continental forearc triggered by the 2010 Maule earthquake, Chile, *Geophysical Journal International*, *188*(3), 879-890.

Scholz, C. H. (1998), Earthquakes and friction laws, *Nature*, *391*(6662), 37-42.

Sun, T., Wang, K., Fujiwara, T., Kodaira, S., and He, J. (2017), Large fault slip peaking at trench in the 2011 Tohoku-oki earthquake, *Nature communications*, *8*(1), 1-8.

Tong, X., Sandwell, D., Luttrell, K., Brooks, B., Bevis, M., Shimada, M., Foster, J., Smalley Jr, R., Parra, H., and Báez Soto, J. C. (2010), The 2010 Maule, Chile earthquake: Downdip rupture limit revealed by space geodesy, *Geophysical Research Letters*, *37*(24).

Tsuji, T., Ito, Y., Kido, M., Osada, Y., Fujimoto, H., Ashi, J., Kinoshita, M., and Matsuoka, T. (2011), Potential tsunamigenic faults of the 2011 off the Pacific coast of Tohoku Earthquake, *Earth, planets and space*, *63*(7), 58.

Wang, K., and He, J. (2008), Effects of frictional behavior and geometry of subduction fault on coseismic seafloor deformation, *Bulletin of the Seismological Society of America*, *98*(2), 571-579.

Wang, K., and Hu, Y. (2006), Accretionary prisms in subduction earthquake cycles: The theory of dynamic Coulomb wedge, *Journal of Geophysical Research: Solid Earth*, *111*(B6).

Wang, X., and Morgan, J. K. (2019), Controls on Fore-Arc Deformation and Stress Switching After the Great 2011 Tohoku-Oki Earthquake From Discrete Numerical Simulations, *Journal of Geophysical Research: Solid Earth, 124*(8), 9265-9279.

Wei, S., Graves, R., Helmberger, D., Avouac, J.-P., and Jiang, J. (2012), Sources of shaking and flooding during the Tohoku-Oki earthquake: A mixture of rupture styles, *Earth and Planetary Science Letters, 333,* 91-100.

Figures

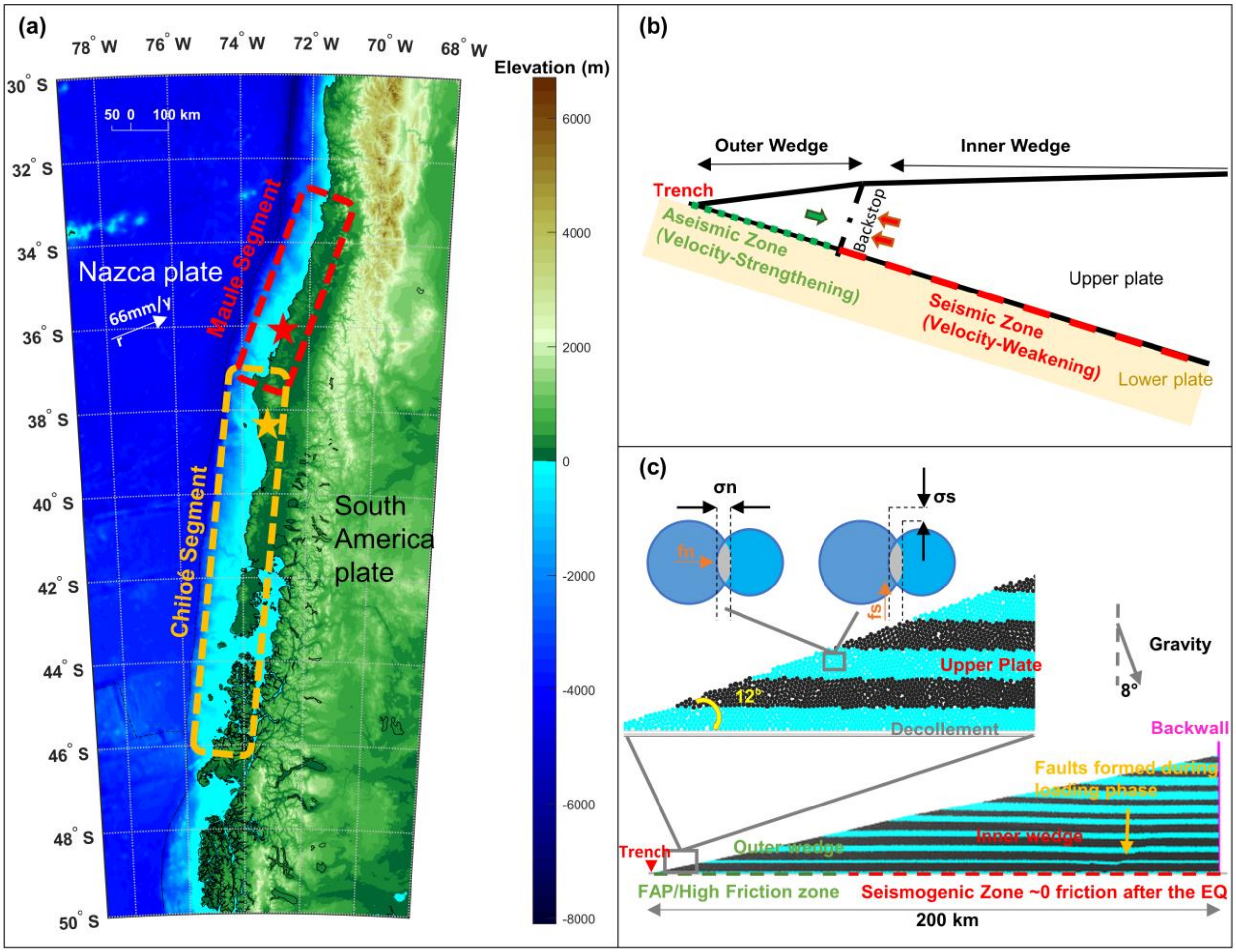

Figure 1 (a) The location map of the South Central (SC) Chile Margin, approximately showing the 1960 Valdivia Earthquake rupture area (yellow ellipse) and the 2010 Maule Earthquake rupture area (red ellipse). The yellow and red rupture areas correlate with the Chiloé and Maule segment, repsectively. (b) Conceptual model for the overriding continental plate consisting of an outer wedge (nominally aseismic zone, green dashed line) and inner wedge (seismic, velocity-weakening zone, red dashed line). (c) DEM model setup of the wedge profile; note that gravity is inclined, introducing a dipping basal surface.

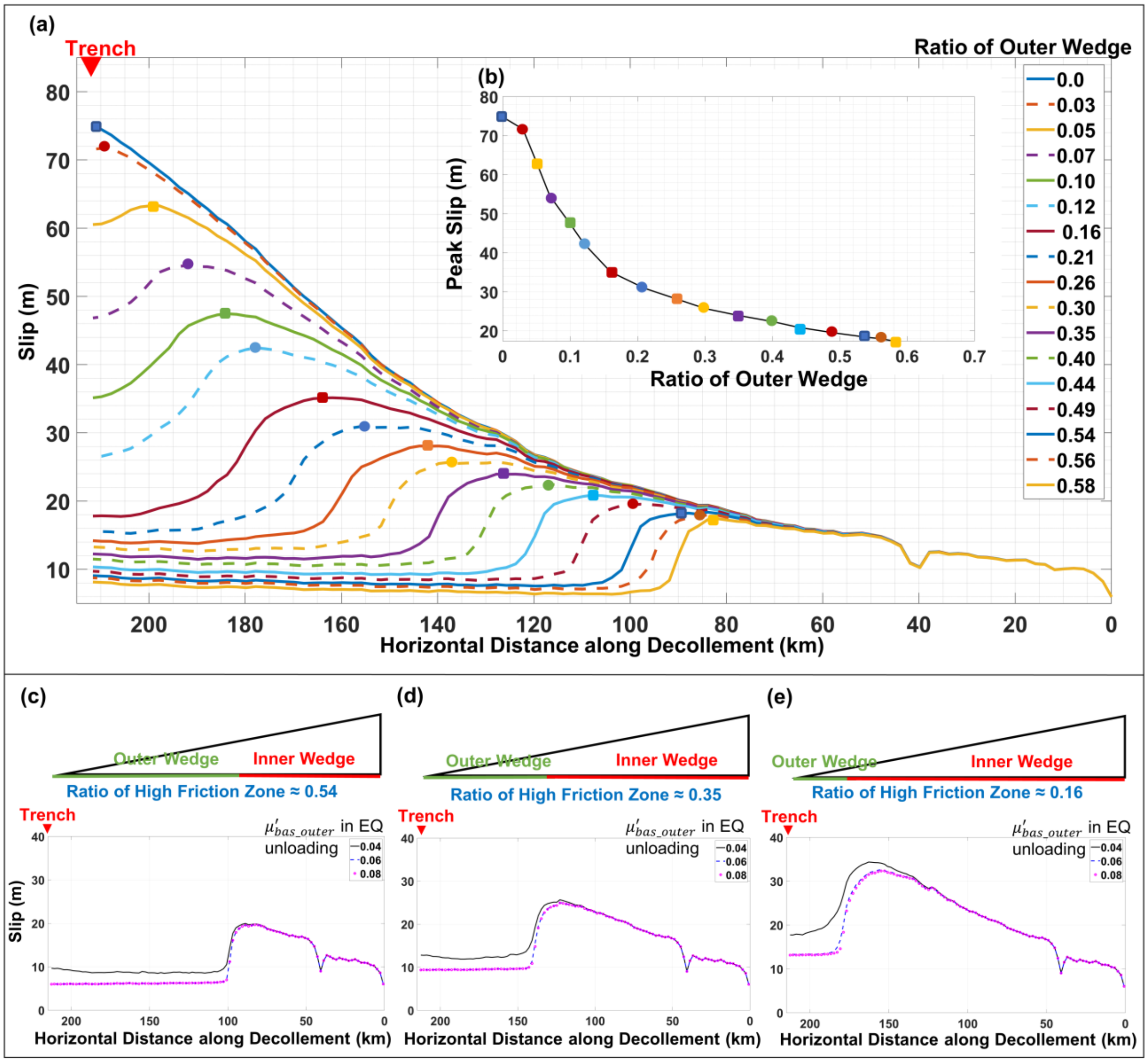

Figure 2 (a) Coseismic slip distributions along the decollement for different ratios of the outer wedge. (b) Peak slip values from the coseismic slip distributions versus outer wedge ratio. Coseismic slip distributions along the decollement for different changes in basal friction beneath the outer wedge for outer wedge ratios of (c) 0.54 (d) 0.35, and (e) 0.16.

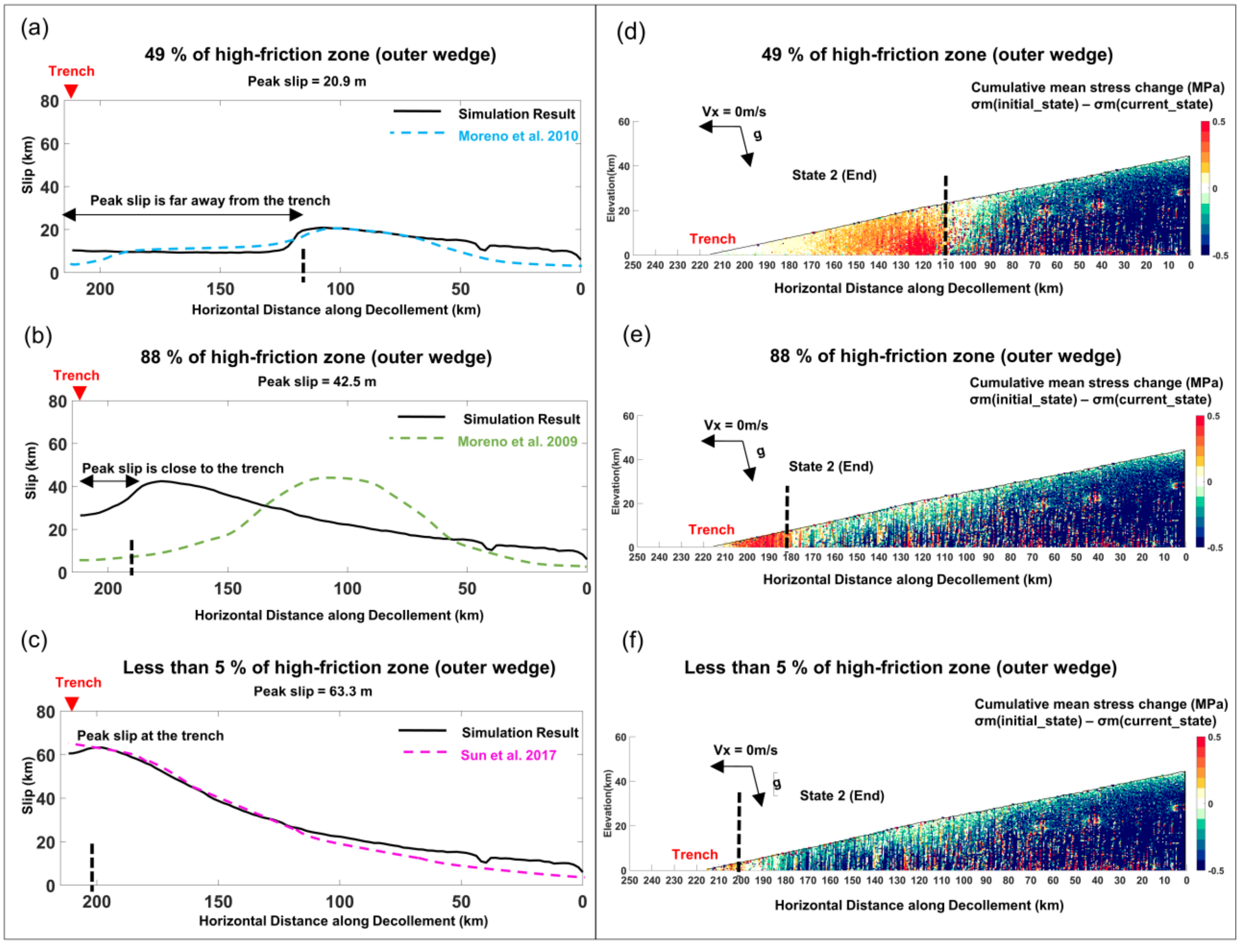

Figure 3. Simulated coseismic slip scenarios compared with derived slip models for the (a) 2010 Maule earthquake rupture (Moreno *et al.*, 2010), (b) 1960 Valdivia earthquake rupture (Moreno *et al.*, 2009), and (c) 2011 Tohoku earthquake rupture (Sun *et al.*, 2017). Simulated coseismic changes in mean stress to demonstrate stress transfer within the wedge for each earthquake: (d) 2010 Maule earthquake, (e) 1960 Valdivia earthquake, and (f) 2011 Tohoku earthquake. Red indicates increase in mean stress blue indicates decrease. The black dashed line locates the boundary between the inner and outer wedges, marking a change in basal friction behavior.